J. Phys. B: At. Mol. Opt. Phys. 28 (1995) 1023–1048. Printed in the UK

Excitation of the 2^3S metastable state of helium by electrons

Surbhi Verma†, Rajesh Srivastava† and Y Itikawa‡

† Department of Physics, University of Roorkee, Roorkee 247 667, India
‡ Institute of Space and Astronautical Science, Yoshinodai, Sagamihara, Japan

Received 7 September 1994

Abstract. A systematic calculation for the total and differential cross sections for electron impact excitation of helium from its initially excited metastable 2^3S state to higher states namely $n^{1,3}S$ and $n^{1,3}P$ (with $n=2$–4) states is reported. Distorted wave approximation theory has been used for the calculation. The effect of different distortion potentials as well as the effect of target polarization by the projectile is explicitly considered. For comparison similar first Born level results are also calculated. Results are compared with the available earlier calculations and experimental data.

1. Introduction

Extensive studies have been carried out on excitation of atoms from their ground state. On the other hand excitation of atoms from their excited states has received relatively less attention. It is well known that the latter process is of equally fundamental importance in many fields of application. Recently the need for a systematic study of the electron impact excitation of atoms in excited states has been emphasized (Lin and Anderson 1992, Trajmar and Nickel 1992, and Burke 1993). Correspondingly the subject has had renewed interest and theoretical calculations, as well as experimental data, are becoming available (Mansky and Flannery 1992, Lockwood *et al* 1992, Krishnan and Stumpf 1992, Christophorou and Illenberger 1993, Verma and Srivastava 1994).

In the present paper, excitation of helium in its 2^3S metastable state is studied theoretically. For this excitation process, some experimental results are already available (Müller-Fiedler *et al* 1984, Rall *et al* 1989, Lockwood *et al* 1992). To compare with these experimental data, several calculations have been attempted (Mathur *et al* 1987, Khurana *et al* 1987, Mansky and Flannery 1992, Franca and da Paixão 1994). Their calculations, however, have only been performed for the transitions 2^3S–2^3P, 3^3S and 3^3P. Though they reported both the differential cross sections (DCS) and the total (i.e. integrated over scattering angles) cross section (TCS), their DCS are limited in the range of small scattering angles (0°–60°), for which only the experimental data are available. Furthermore the agreement between the experimental and the theoretical values is not necessarily convincing. Berrington *et al* (1985) made an 11 state R-matrix calculation for He. They obtained cross sections for the transitions 2^3S–n^3L, n^1L with $n=2$, 3 and $L \leqslant n-1$. Their calculation, however, was carried out only at a collision energy of less than 10 eV. For the transitions among the $n=2$ states, two more calculations have been reported (Fon *et al* 1981, Badnell 1984). They reported no DCS. Considering this situation of the available data on the excitation of He(2^3S) (also see the recent compilation

0953-4075/95/061023+26$19.50

of TCS for He by Kato *et al* (1992)), we have made a more comprehensive calculation: both TCS and DCS have been calculated for the transitions 2^3S–n^3L, n^1L with $n=2$–4 and $L=0$, 1 over the energy range 10–100 eV.

The present calculation is based on the distorted wave approximation (DWA). Three different types of distortion potential are used to test the dependence of the resulting cross section on the choice of the distortion potential. The effect of the target polarization is also investigated. A comparison with the experimental data and other calculations is made as far as possible. Born–Ochkur and Born–Oppenheimer approximation results are obtained for 2^3S–n^1L transitions.

2. Theory

In the first-order distorted wave approximation the transition matrix for the electron impact excitation of helium from its initial state 'i' to a final state 'f' can be written as (atomic units are used throughout)

$$T_{if} = \langle \chi_f^- | V - U_f | A \chi_i^+ \rangle \tag{1}$$

where A is the antisymmetrization operator which takes into account electron exchange between projectile and target electrons. V is the total interaction potential given by

$$V = -\frac{2}{r_3} + \frac{1}{|r_1 - r_3|} + \frac{1}{|r_2 - r_3|} \tag{2}$$

where r_1, r_2 and r_3 are respectively the position coordinates of the two target electrons and the projectile electron with respect to the nucleus of the target. $\chi_i^+(\chi_f^-)$ is the combined wavefunction of the incident electron and the electrons in the initial (final) state of He. It is defined as

$$\chi_{i(f)}^{+(-)} = F^{+(-)}[k_{i(f)}, r_3]\psi_{i(f)}(r_1, r_2)S_{i(f)}(1, 2; 3) \tag{3}$$

where $\psi_{i(f)}$ is the initial (final) target helium atom wavefunction and $S_{i(f)}(1, 2; 3)$ is the initial (final) state spin function for the composite system consisting of the incident projectile and the target. $F_{i(f)}^{+(-)}$ represents the initial (final) channel projectile distorted wave with the wavevector $k_i(k_f)$ and the associated superscript $+(-)$ indicates the usual outgoing (incoming) wave boundary condition. These distorted waves are the solutions of

$$[\nabla_3^2 + k_{i(f)}^2 - 2U_{i(f)}(r_3)]F^{+(-)}(k_{i(f)}, r_3) = 0. \tag{4}$$

The $U_{i(f)}$ is the distortion potential, the exact form of which is defined below.

On substituting χ_i^+ and χ_f^- in equation (3) into the T-matrix (equation (1)) we get

$$\begin{aligned} T_{i(f)} = {} & \langle F^-(k_f, r_3)\psi_f(r_1, r_2)S_f(1, 2; 3)| V - U_f | F^+(k_i, r_3)\psi_i(r_1, r_2)S_i(1, 2; 3)\rangle \\ & - 2\langle F^-(k_f, r_3)\psi_f(r_1, r_2)S_f(1, 2; 3)| V - U_f | \\ & \times F^+(k_i, r_1)\psi_i(r_3, r_2)S_i(3, 2; 1)\rangle. \end{aligned} \tag{5}$$

This equation can be simplified further for a specific transition by carrying out the integrations over the spin coordinates. Basically we consider two types of transitions: namely triplet to triplet (TT) and triplet to singlet (TS) excitations. In the following section we give a brief outline how to evaluate the T-matrix for each TT and TS excitation process.

2.1. Triplet–triplet excitations ($2^3S \rightarrow n^3L$ with $L=0, 1$)

In the triplet–triplet excitation the scattering can take place with the total spin S of the system being $\frac{1}{2}$ or $\frac{3}{2}$ i.e. either in the doublet mode (D) or in the quartet mode (Q). The spin functions in these modes are referred to as $S_{D,Q}(1, 2; 3)$. Scattering in a doublet mode occurs in one third of all collisions while two thirds of all collisions are in a quartet mode. The quartet normalized spin function $S_Q(1, 2; 3)$ in terms of usual Dirac matrices α and β for the three electron system with total magnetic components $M_s=\frac{3}{2}$ and $\frac{1}{2}$ is given by (Schiff 1968)

$$S_Q(1, 2; 3) = \alpha_1\alpha_2\alpha_3 \qquad M_s=\tfrac{3}{2}$$

$$= \frac{1}{\sqrt{3}}(\alpha_1\alpha_2\beta_3 + \alpha_1\beta_2\alpha_3 + \beta_1\alpha_2\alpha_3) \qquad M_s=\tfrac{1}{2} \tag{6}$$

and the doublet spin function $S_D(1, 2; 3)$ for the total magnetic component $M_s=\frac{1}{2}$ is given by

$$S_D(1, 2; 3) = \frac{1}{\sqrt{6}}[2\alpha_1\alpha_2\beta_3 - \alpha_3(\alpha_1\beta_2 + \alpha_2\beta_1)]. \tag{7}$$

Substituting S_Q into both S_i and S_f in equation (5) and carrying out the spin integrations using the orthogonal properties of individual spin functions i.e.

$$\begin{aligned} &\langle\alpha_i|\alpha_j\rangle = \delta_{ij} \\ &\langle\beta_i|\beta_j\rangle = \delta_{ij} \\ &\langle\alpha_i|\beta_j\rangle = 0 \end{aligned} \tag{8}$$

we get

$$T^{(1)} = T^d - 2T^{ex}. \tag{9}$$

Similarly, if the scattering is taking place in the doublet mode i.e. $S_i = S_f = S_D$, we get after the spin integrations

$$T^{(2)} = T^d + T^{ex}. \tag{10}$$

In equations (9) and (10) T^d and T^{ex} are the spin averaged direct and exchange T-matrices given by

$$T^d = \int F^-(\boldsymbol{k}_f, \boldsymbol{r}_3)\psi_f(\boldsymbol{r}_1, \boldsymbol{r}_2)(V - U_f(\boldsymbol{r}_3))F^+(\boldsymbol{k}_i, \boldsymbol{r}_3)\psi_i(\boldsymbol{r}_1, \boldsymbol{r}_2)\, d\boldsymbol{r}_1\, d\boldsymbol{r}_2\, d\boldsymbol{r}_3 \tag{11}$$

$$T^{ex} = \int F^-(\boldsymbol{k}_f, \boldsymbol{r}_3)\psi_f(\boldsymbol{r}_1, \boldsymbol{r}_2)(V - U_f(\boldsymbol{r}_3))F^+(\boldsymbol{k}_i, \boldsymbol{r}_1)\psi_i(\boldsymbol{r}_3, \boldsymbol{r}_2)\, d\boldsymbol{r}_1\, d\boldsymbol{r}_2\, d\boldsymbol{r}_3. \tag{12}$$

Thus the differential cross section for the triplet–triplet excitations is given by

$$\left|\frac{d\sigma}{d\Omega}\right|_{TT} = \frac{1}{4\pi^2}\frac{\boldsymbol{k}_f}{\boldsymbol{k}_i}[\tfrac{1}{3}|T^{(1)}|^2 + \tfrac{2}{3}|T^{(2)}|^2]. \tag{13}$$

2.2. Triplet–singlet excitations ($2^3S \rightarrow n^1L$, with $L=0, 1$)

In the triplet–singlet excitations the scattering can take place only in the doublet mode i.e. the total spin of the system $S=\frac{1}{2}$. This is because of the conservation of the total

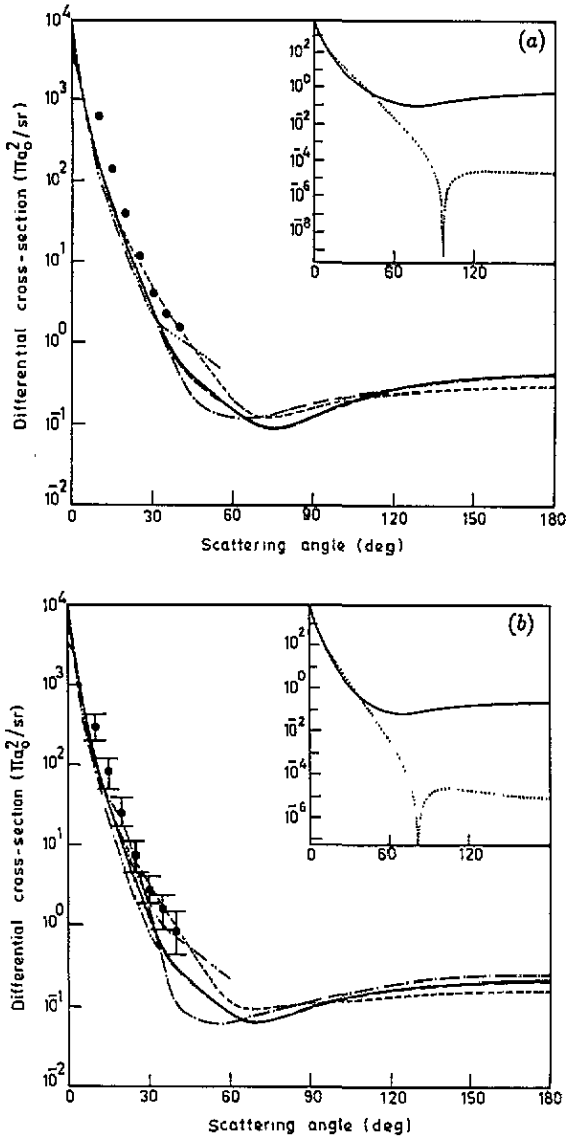

Figure 1. DCS (πa_0^2/sr) for the 2^3S–2^3P excitation of helium. (*a*) At final electron energy $E_f = 15$ eV. (——) Present FF; (-----) present IIP; (– – –) present II; (· · · ·) Present FBA; (– · · · –) DWA results of Mathur *et al* (1987); (– · – · –) FOMBT results of Csanak *et al* (1994); (●) experimental results of Müller-Fiedler *et al* (1984). (*b*) As in figure 1(*a*) but for $E_f = 20$ eV and (– · · – · · –) DMET results of Mansky and Flannery (1992). (*c*) As in figure 1(*a*) but for $E_f = 30$ eV.

spin of the system during the excitation process. The expressions for S_i and S_f in the TS excitation are given by

$$S_i = \frac{1}{\sqrt{6}}[2\alpha_1\alpha_2\beta_3 - \alpha_3(\alpha_1\beta_2 + \alpha_2\beta_1)] \tag{14}$$

$$S_f = \frac{1}{\sqrt{2}}[\alpha_1\beta_2 - \alpha_2\beta_1]\alpha_3. \tag{15}$$

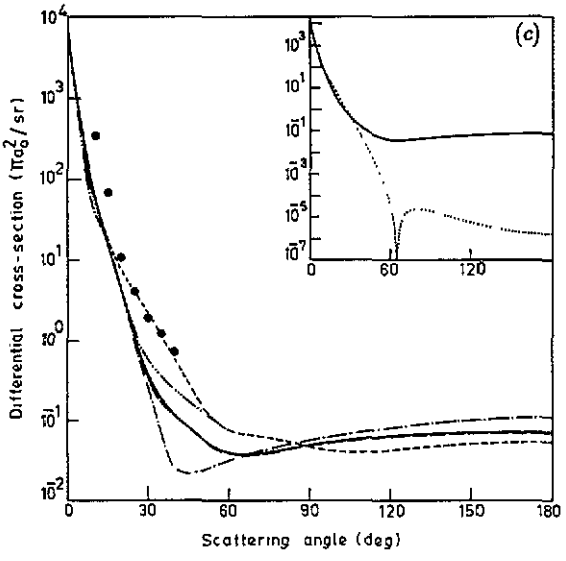

Figure 1. (continued)

On substituting these in the T-matrix (equation (5)) and carrying out the spin integrations we get

$$T^{(3)} = \sqrt{3}\, T^{\mathrm{ex}}. \tag{16}$$

The direct transition matrix T^{d} does not appear because the TS excitation cannot take place without an interchange of the projectile and target electron.

Consequently the differential cross section for the TS excitation in helium atom is given by

$$\left|\frac{\mathrm{d}\sigma}{\mathrm{d}\Omega}\right|_{\mathrm{TS}} = \frac{1}{4\pi^2}\frac{k_{\mathrm{f}}}{k_{\mathrm{i}}}|T^{(3)}|^2. \tag{17}$$

2.3. Choice of wavefunctions

In order to evaluate integrals (equations (11) and (12)), we require the wavefunctions for helium in its initial and final states. For this purpose the Hartree–Fock wavefunctions have been used for the bound states of the target helium atom. These are the one-configuration variational wavefunctions derived and used by Winter and Lin (1975) and have the following form for the relevant $n^{1,3}L$ states

$$\psi(n^{1,3}LM|r_1, r_2) = [N(n^{1,3}L)/\sqrt{2}]\{\phi_2(n^{1,3}LM|r_1)\phi_1[Z|r_2] \pm \phi_1[Z|r_1]\phi_2(n^{1,3}LM|r_2)\}$$

with

$$\phi_2(n^{1,3}LM|r) = r^L Y_{LM}(\hat{r}) \exp[-a(n^{1,3}L)r] \sum_{k=1}^{n-L} (-1)^{k-1} b(n^{1,3}L, k) r^{k-1} \tag{18}$$

and the wavefunction of the 1s electron

$$\phi_1(Z|r) = (Z^3/\pi)^{1/2} \exp(-Zr) \tag{19}$$

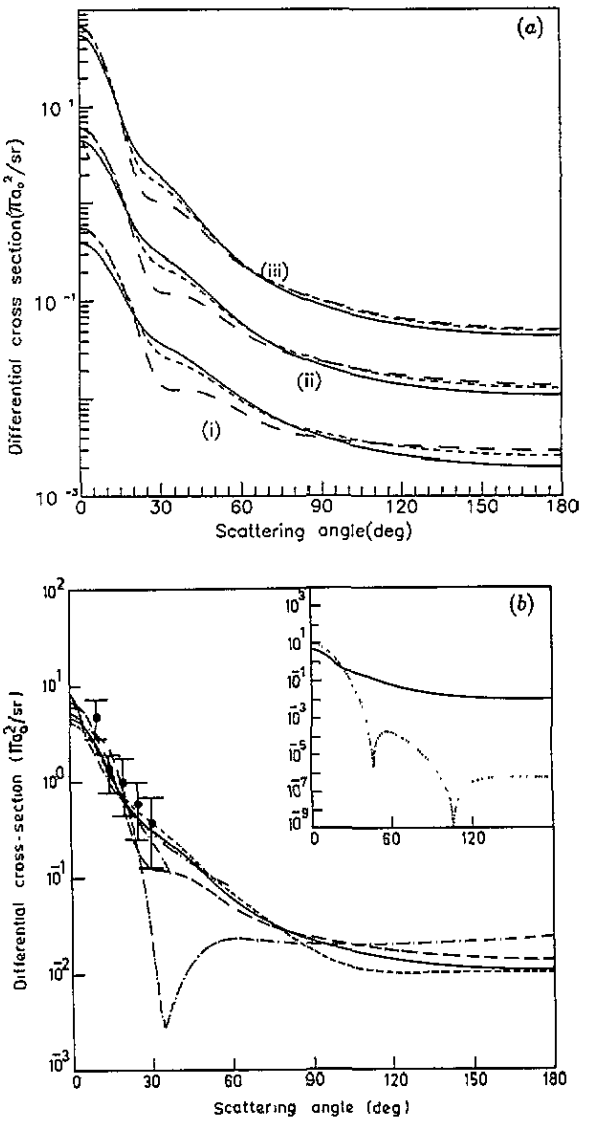

Figure 2. DCS (πa_0^2/sr) for the 2^3S–3^1S excitation of helium. (*a*) Comparison of present results at (i) 15 eV, (ii) 20 eV, (iii) 30 eV. (——) FF; (-----) IF; (- - -) II; the results at $E_f = 15$ and 30 eV have been multiplied by 0.1 and 10 respectively. (*b*) As in figure 1(*b*).

with $Z=2$. The parameters a, b and N occurring in ϕ_2 have been taken from the paper of Winter and Lin (1975). The helium wavefunctions $\psi(n^{1,3}L|r_1, r_2)$ for all n are orthonormalized to each other. Further all the one-electron wavefunctions $\phi_2(n^{1,3}L|r)$ have been set orthonormalized to one another and to the ground-state wavefunction $\phi_1(Z|r)$ of the helium ion.

2.4. Choice of distorting potential

To obtain the distorted wave for the initial (final) channel (from equation (4)) we need a suitable distortion potential $U_{i(f)}$. Here we introduce the distortion potential in the

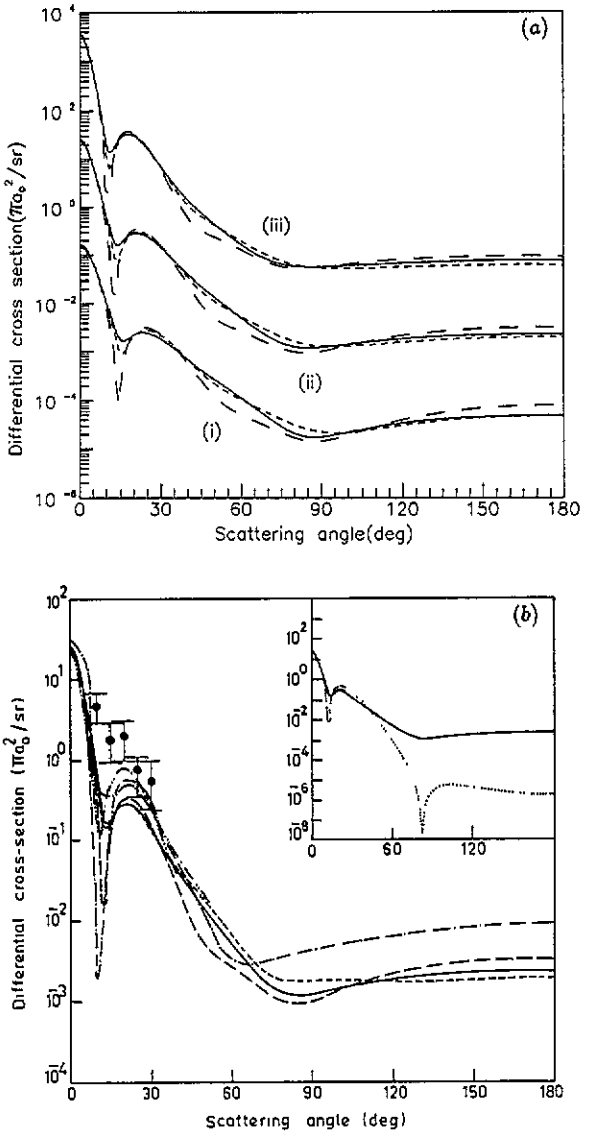

Figure 3. DCS (πa_0^2/sr) for 2^3S-3^3P excitation in helium. (*a*) Same as figure 2(*a*) except that the results at $E_f = 15$ eV and 30 eV have been multiplied by 0 01 and 100 respectively. (*b*) As in figure 2(*b*).

form

$$U_{i(f)} = V_a^{stat} + V_{i(f)}^{exch} + V_{i(f)}^{pol} \quad (\text{with } a = \text{i or f}). \tag{20}$$

V_a^{stat} is the spherically averaged static potential of the helium atom in the initial (a=i) or final (a=f) state i.e.

$$V_a^{stat} = \langle \phi_a | V | \phi_a \rangle. \tag{21}$$

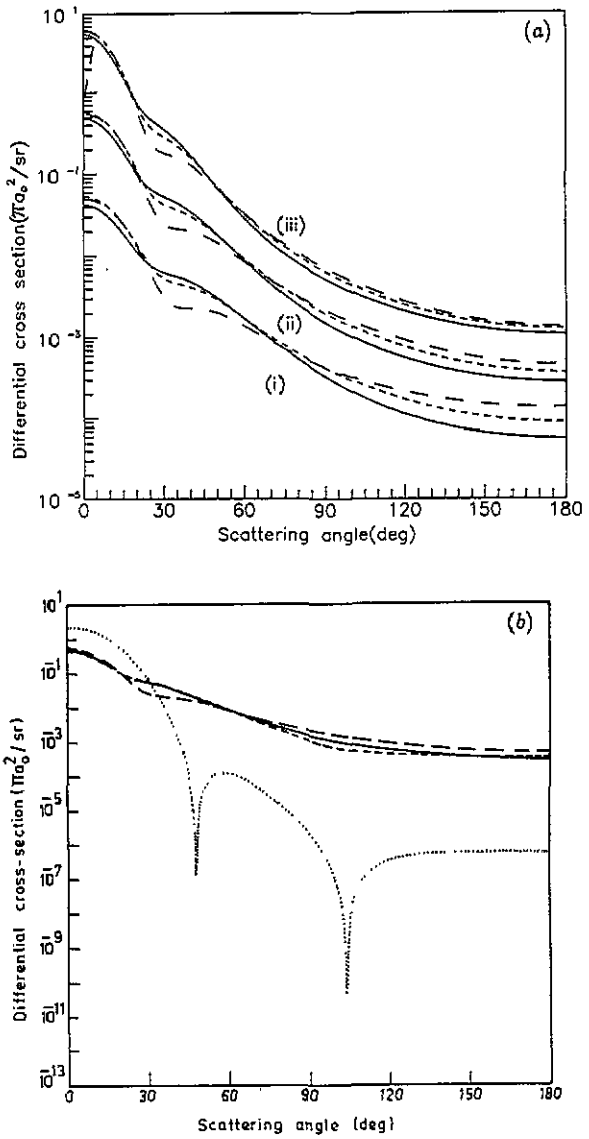

Figure 4. DCS (πa_0^2/sr) for 2^3S-4^3S excitation in helium. (*a*) As in figure 2(*a*); (*b*) as in figure 2(*b*).

$V_{i(f)}^{exch}$ is the exchange distortion potential in the initial (final) channel and is taken to be that of Furness and McCarthy (1973)

$$V_{i(f)}^{exch} = \tfrac{1}{2}\{(\tfrac{1}{2}k_{i(f)}^2 - V_a^{stat}) - [(\tfrac{1}{2}k_{i(f)}^2 - V_a^{stat})^2 - 8\pi\tau\rho_a]^{1/2}\}. \tag{22}$$

Here ρ_a is the spherical average of the one electron charge density of the helium atom in the initial or final channel. The value of the parameter τ depends on the total spin of the colliding system and is taken from the paper by Vučić *et al* (1987). For the channel $e + He(n^3L)$, it takes -1 for the doublet system and $+2$ for the quartet one. For $e + He(n^1L)$, $\tau = 1$. The above form (equation (22)) is, in fact, one of the best local approximations for the exchange potential for the region of intermediate electron energy

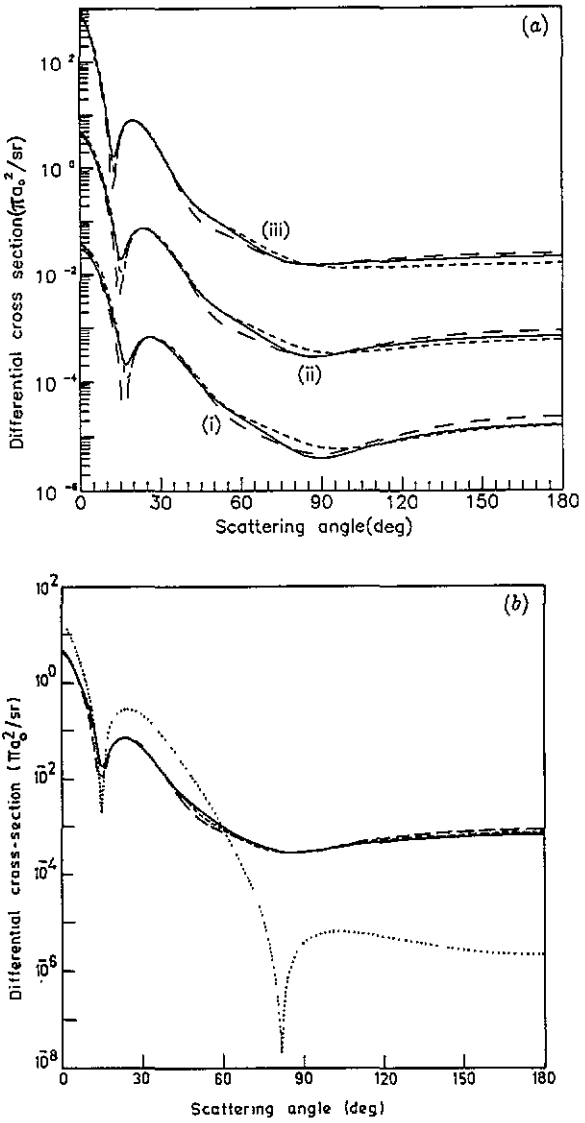

Figure 5. DCS (πa_0^2/sr) for 2^3S–4^3P excitation in helium. (*a*) As in figure 3(*a*); (*b*) as in figure 4(*b*).

and has been widely used. Further in order to obtain V^{stat} and ρ we use the same target wavefunction as for the evaluation of the T matrix. The polarization potential is described in the next section.

In the DWA calculation, an arbitrariness remains on the choice of the distortion potential in each channel. In principle we can choose the distortion potential in any mathematical from (Itikawa 1986, Katiyar and Srivastava 1989, Madison *et al* 1991). The most straightforward calculation is that the incoming electron is distorted by the initial state potential U_i and the outgoing electron is distorted by the final state one U_f (Mott and Massey 1965). Hereafter this choice is referred to as the IF model. A number of previous DWA calculations (see Madison *et al* 1991) suggest that the use of either the

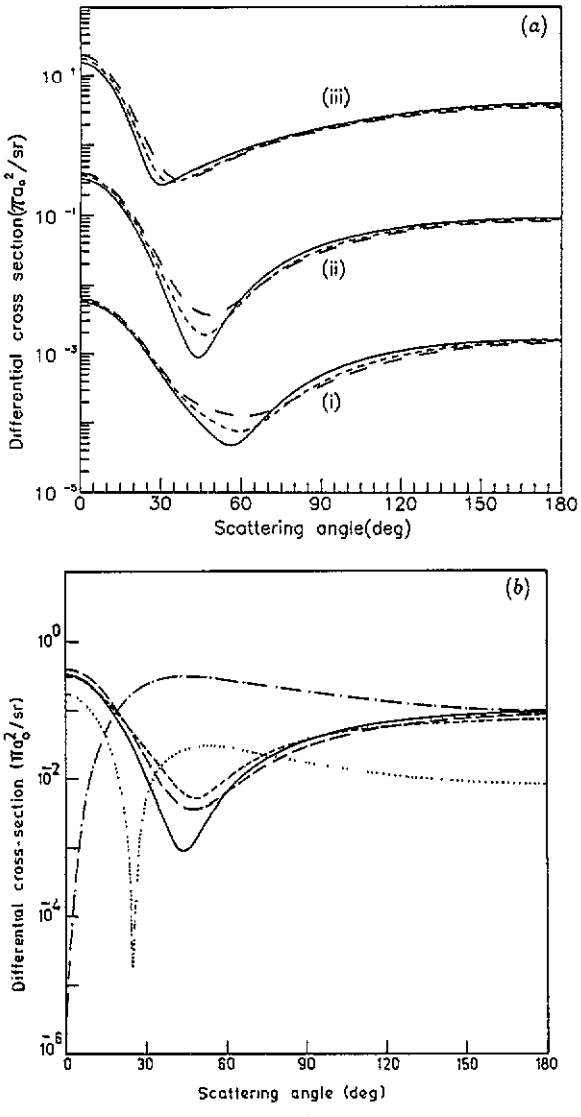

Figure 6. DCS (πa_0^2/sr) for the 2^3S–2^1S excitation in helium. (*a*) As in figure 3(*a*); (*b*) as in figure 2(*b*) and (· · · ·) present BOA; (— · —) present OA.

ground-state distortion potential U_i (II model) or the excited-state distortion potential U_f (FF model) in both the channels yields results in better agreement with experimental data. We have carried out the three separate sets of calculations i.e. using the IF, II and FF models of the potential to explore their suitability for the present problem.

2.5. *Choice of polarization potential*

The choice of the polarization potential is mostly done in an empirical or phenomenological way and therefore several forms of polarization potentials are available in the literature (see for example Nakanishi and Schrader 1986). For the present calculation

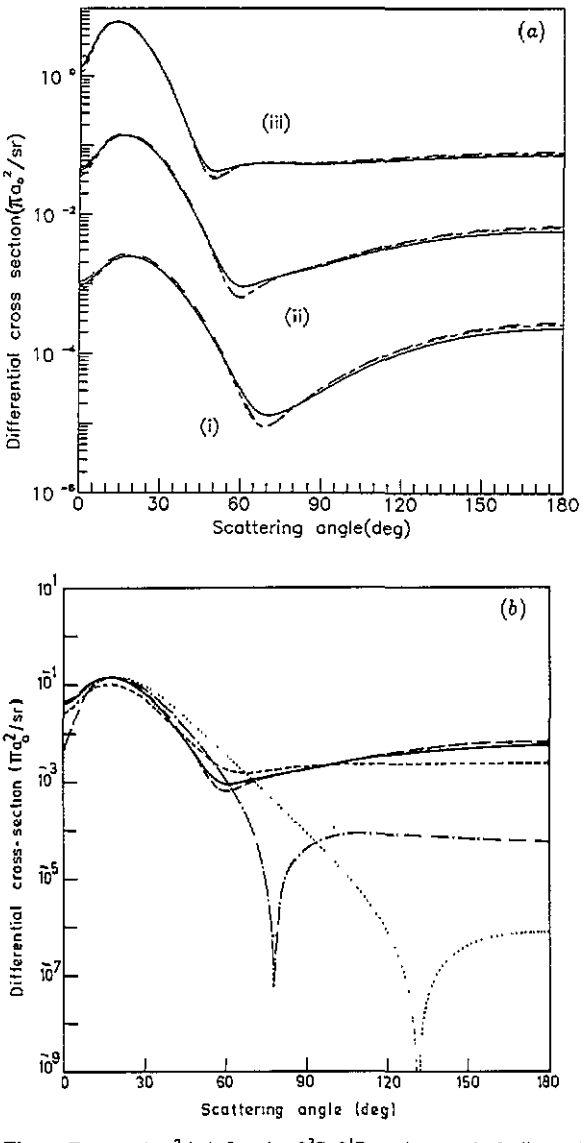

Figure 7. DCS (πa_0^2/sr) for the 2^3S–2^1P excitation in helium. (*a*) As in figure 6(*a*); (*b*) as in figure 6(*b*).

we adopt the widely used simple Buckingham type polarization potential proposed by Jhanwar and Khare (1976) namely

$$V_j^{\text{pol}} = -\frac{\alpha_d r^2}{2(r^2+d^2)^3} \tag{23}$$

where α_d is the static dipole polarizability of the atom in the jth state (see Miller and Bederson 1977). The parameter d is chosen in the literature in a variety of ways. In the present paper we use the value of d as taken and used by Mittleman and

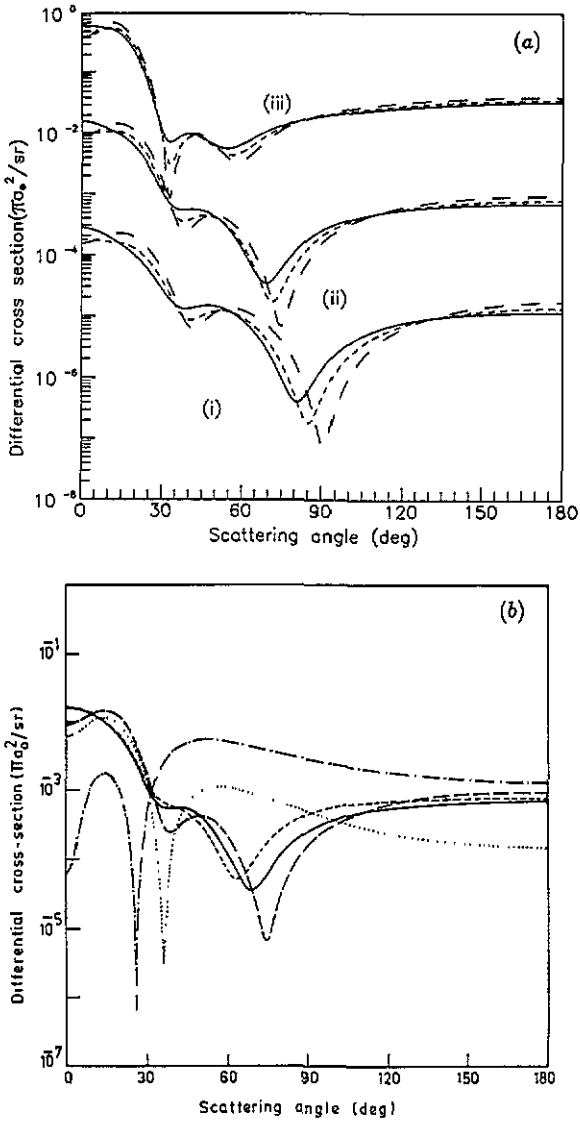

Figure 8. DCS (πa_0^2/sr) for the 2^3S–3^1S excitation in helium. As in figure 7.

Watson (1960)

$$d=(\tfrac{1}{2}\alpha_d\beta^2Z^{-1/3})^{1/4}. \tag{24}$$

We consider β as an adjustable (energy dependent) parameter as taken by Salvat *et al* (1987) and many others. Here Z is the nuclear charge of helium.

The parameter β is varied with energy in such a manner that the calculated theoretical result is in best agreement with the available experimental data for 2^3S–2^3P, -3^3S and -3^3P excitations. For other transitions, where no experimental data are available, we take it energy independent as taken by Mittleman and Watson (1960) and use $\beta=1$. We consider the effect of polarization only in the II model. For He (2^3S), we have $\alpha_d=315$ (Christophorou and Illenberg 1993) but for other excited states nothing is

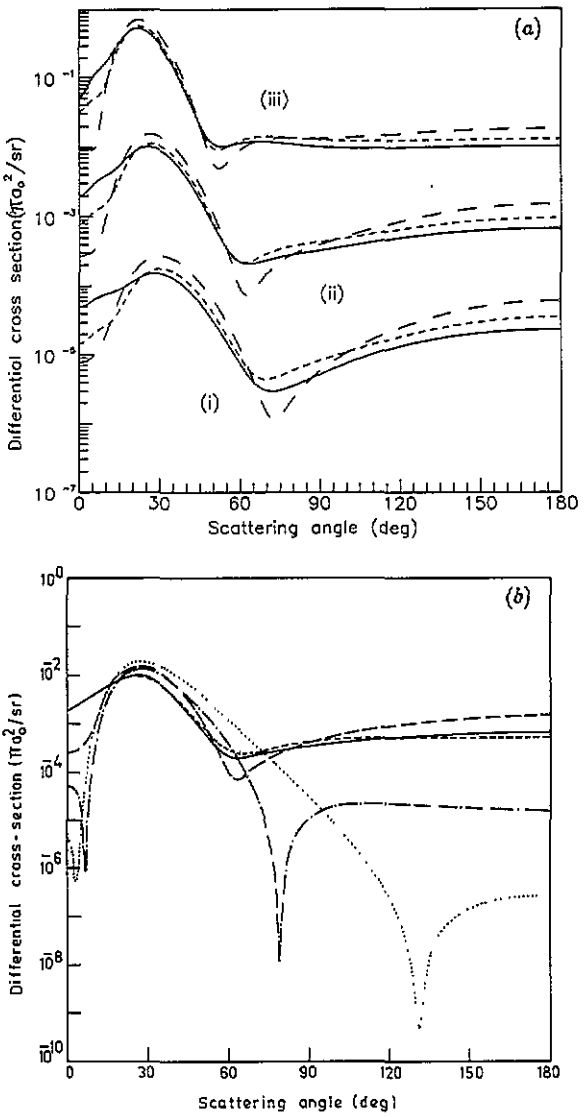

Figure 9. DCS (πa_0^2/sr) for the 2^3S–3^1P excitation in helium. As in figure 7.

known about α_d. This is the reason why we do not study the effect of polarization in the IF and FF models.

3. Results and discussions

Using our DWA method described in the previous section, the DCS and TCS are obtained for excitation from the 2^3S state of helium to the higher excited $n^{1,3}S$ and $n^{1,3}P$ states with $n \leqslant 4$. The calculation is made in the three different versions of the DWA method, i.e. the II, IF and FF models. For the triplet–triplet excitations the first Born approximation (FBA) is also calculated, while for the triplet–singlet excitations the calculations

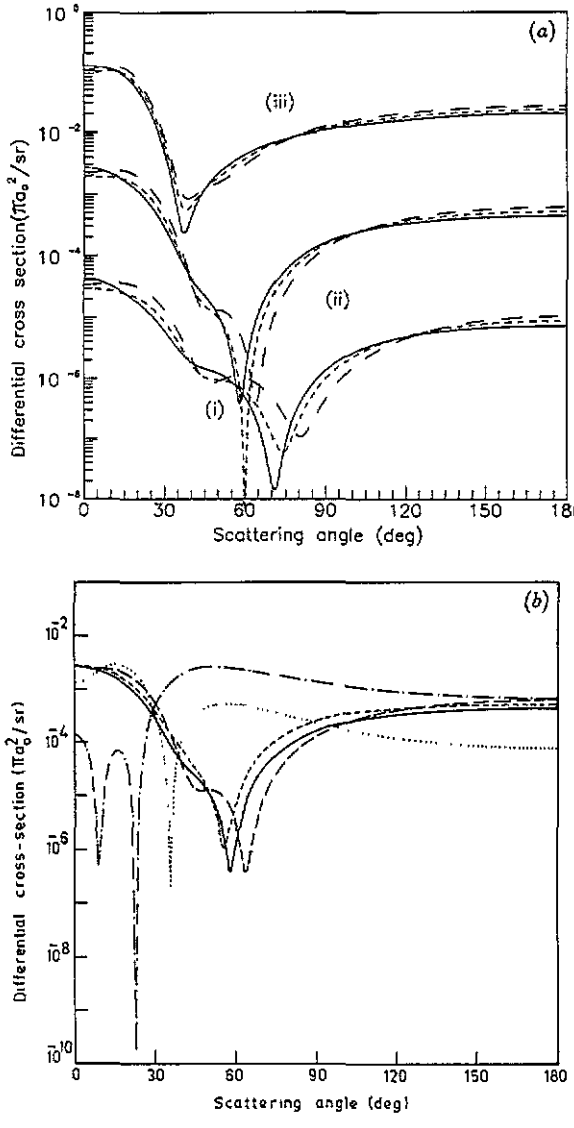

Figure 10. DCS (πa_0^2/sr) for the 2^3S–4^1S excitation in helium. As in figure 7.

with the Born–Oppenheimer approximation (BOA) and the Ochkur approximation (OA) are performed. For these FBA, BOA and OA calculations, we employ the same wavefunction as we use for the DWA calculation so that a meaningful comparison can be made. As is mentioned in the previous section, we incorporate the polarization effect in our II model only and the results with polarization are referred to as IIP.

3.1. Differential cross section

3.1.1. Triplet–triplet excitations. Figure 1 compares the present DCS for the 2^3S–2^3P excitation to the experimental data by Müller-Fiedler *et al* (1984) and other theoretical results. The DCS are shown at the final electron energies 15, 20 and 30 eV, at which the

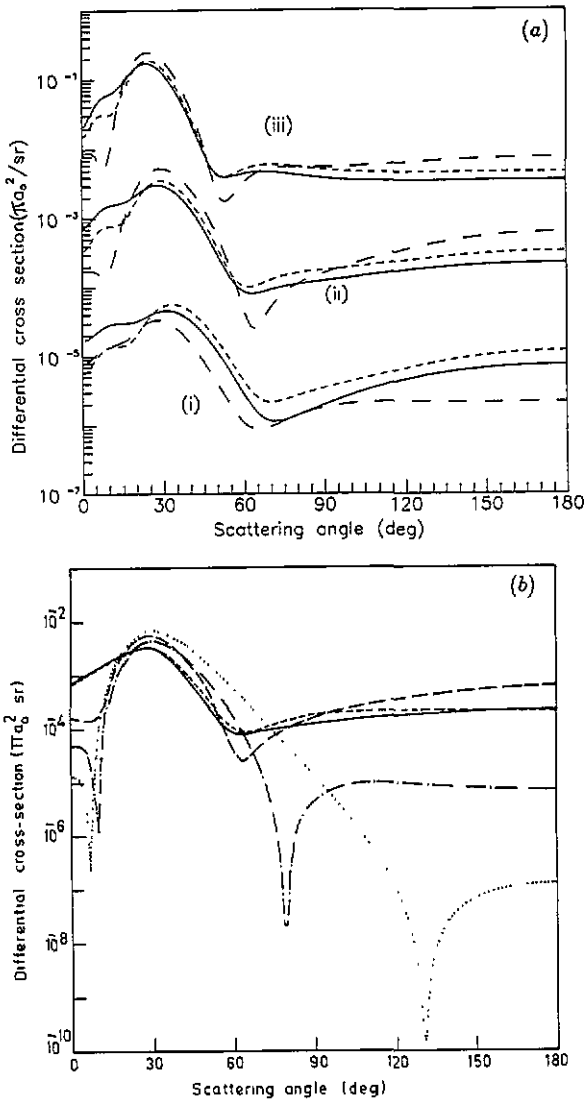

Figure 11. DCS (πa_0^2/sr) for the 2^3S–4^1P excitation in helium. As in figure 7.

experimental data are available. The error bars in the data are plotted only at the final energy of 20 eV, because Müller-Fiedler *et al* have given the error bars of individual data points only at this energy.

In this figure, we show our DWA cross sections in the models II, FF and IIP. As is shown in figures 2 and 3, the FF cross section is in the best agreement with experiment. In most cases, the IF cross section has a magnitude in between those of the II and FF models. For the calculation in the IIP model, the cut-off parameter in the polarization potential has been chosen to give the best agreement with the experimental data. In figure 1, comparisons are made to the theoretical calculations with the multi-channel eikonal theory (DMET) of Mansky and Flannery (1992), the distorted wave approximation (DWA) of Mathur *et al* (1987) and the first-order many-body theory (FOMBT) of Csanak *et al* (1994). It should be noted that our DWA calculation in the IF model is

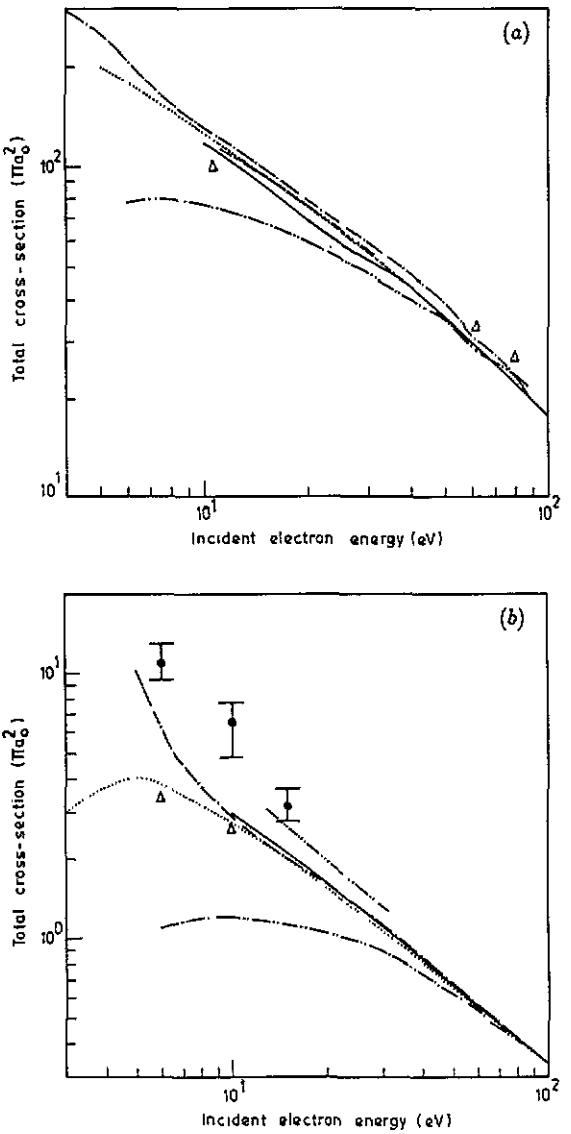

Figure 12. (*a*) TCS (πa_0^2) for the 2^3S–2^3P excitation of helium. (——) Present FF; (· · · ·) present FBA; (– · · · –) DWA results of Mathur *et al* (1987); (– · · –) DMET results of Mansky and Flannery (1992); (– – –) FOMBT results of Csanak *et al* (1994); (△) *R*-matrix results of Fon *et al* (1981). (*b*) TCS (πa_0^2) for 2^3S–3^3S excitation of helium. As in figure 12(*a*) and (△) *R*-matrix results of Berrington *et al* (1985); (●) experimental results of Rall *et al* (1989); (*c*) TCS (πa_0^2) for 2^3S–3^3P excitation in helium. As in figure 12(*b*).

similar to that of Mathur *et al* (1987). However, they gave results only at a limited range of angles and for a few transitions. Further they used different wavefunctions from the present one. After the completion of the present calculation, Franca and da Paixão (1994) reported their FOMBT calculation. In principle their calculation should be the same as that of Csanak *et al* (1994), though, they do not explicitly indicate so.

All the theoretical results agree with each other at angles less than about 30°. In that region, the agreement between theory and experiment is also good. The best

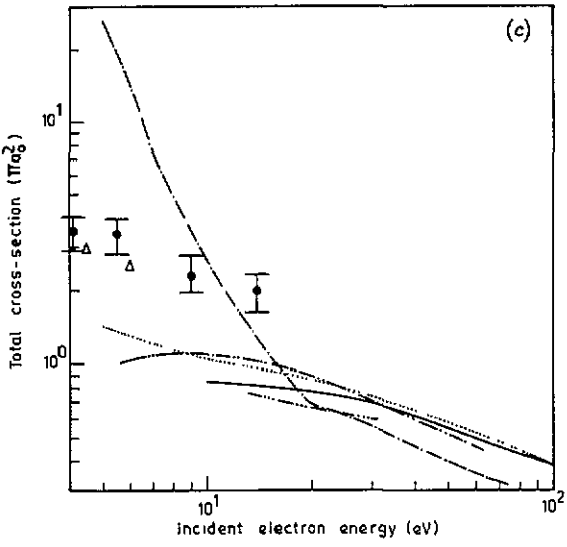

Figure 12. (continued)

agreement with experiment is achieved by the present calculation in the IIP model (i.e. the II model taking account of polarization interaction). It should be noted, however, that this model includes one parameter adjusted to give the best agreement with the experimental data. We also find that there is no significant difference in the results for the three versions for this transition at the considered electron energies. In the inset of the figure, we compare our DWA results with the FBA calculation. The FBA gives DCS in accordance with the DWA calculation only at the very small scattering angles.

Figure 2 presents the DCS for the 2^3S–3^3S excitation. In figure 2(*a*) we compare our results in the three models with each other at the final energies of 15, 20 and 30 eV. As seen from the figure, our three models (i.e. II, IF and FF) give different values of DCS at scattering angles larger than 20°. In particular the II model gives a discernible shoulder in the range 20–30°. This shoulder is shifted towards the small angular side with increasing energy. In figure 2(*b*) we compare our results in the FF, II and IIP models with other available results. The latter are the experimental data of Müller-Fiedler *et al* (1984) and the theoretical values of Mansky and Flannery (1992), Mathur *et al* (1987) and Csanak *et al* (1994). There is a good overall agreement between the present (FF or IIP) calculation and the experimental data. In particular, the shoulder at about 30° in our II model and the FOMBT is absent in the experimental result. In this sense, our FF (and IIP) model gives a better result. (In this case also, the adjustable parameter in the IIP model is chosen to give the best agreement with experiment.) Again the FBA gives very different DCS from the DWA values.

Figure 3 presents the DCS for the 2^3S–3^3P transition. First, in figure 3(*a*), we show the results in our three models at the final energy of 15, 20 and 30 eV. It is seen from the figure that there is a dip in the DCS in the range 10–20°. The largest dip is obtained in the II model. In figure 3(*b*), the results of our calculation in the II, FF and IIP (with the parameter adjusted to give the best agreement with experiment) are compared with the data similar to those in figure 2(*b*). All the theoretical results show a dip in the cross section at about 20°. The experimental data show a slight dip in the same region of angles, but their absolute values are well above all the calculations presented. It is

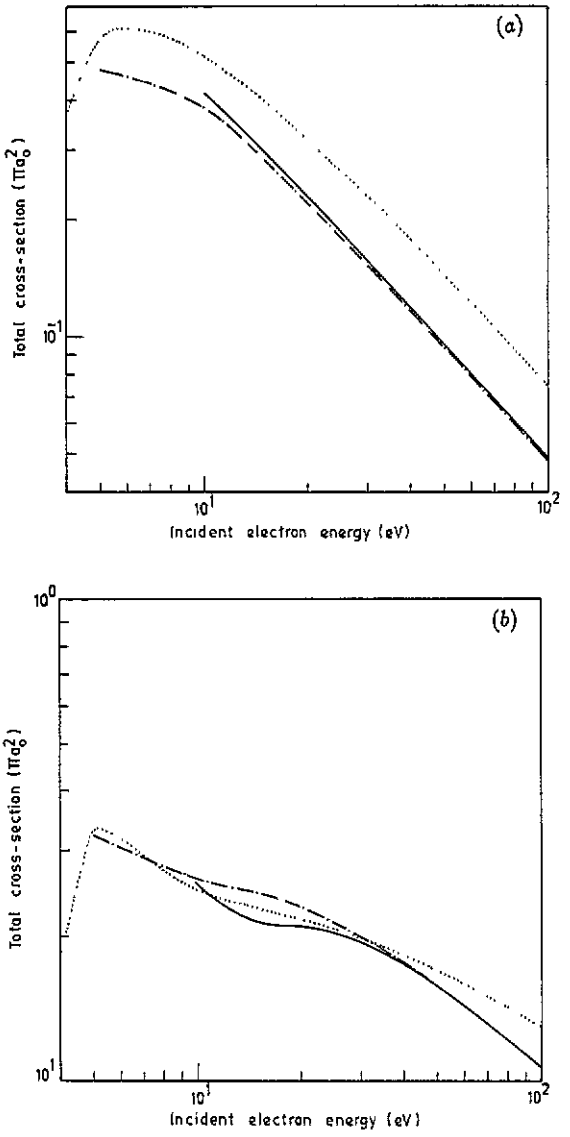

Figure 13. (*a*) TCS (πa_0^2) for 2^3S–4^3S excitation in helium. (——) Present FF results; (- - - -) present OA; (· · · ·) present FBA. (*b*) As in figure 13(*a*) but for 2^3S–4^3P excitation.

interesting to note that the FBA gives two dips, one of which is located also in the vicinity of 20°.

In figures 4 and 5, we show the present results for the transitions 2^3S–4^3S and 2^3S–4^3P, respectively. There are neither theoretical nor experimental data to compare with. It should be noted here that the qualitative angular dependence for the excitation of 4^3S is very similar to that for 3^3S (figure 2). Also we can see similar resemblance between the DCS for 4^3P and 3^3P. The absolute magnitude of the DCS for the excitation of the $n=4$ states, however is smaller by almost one order of magnitude than that for the $n=3$ states.

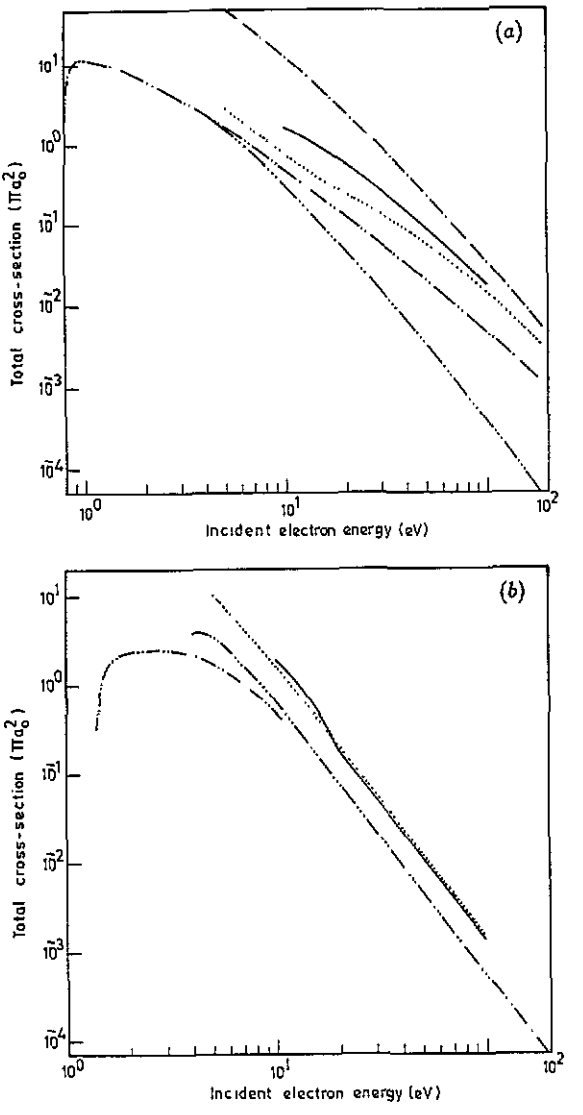

Figure 14. (*a*) TCS (πa_0^2) for 2^3S–2^1S excitation in helium. (——) Present FF results; (· · · ·) present BOA; (- - - -) present OA; (– · · · –) *R*-matrix results of Fon *et al* (1981); (– · – · –) *R*-matrix results of Badnell (1984). (*b*) As in figure 14(*a*) but for 2^3S–2^1P excitation.

3.1.2. Triplet–singlet excitations. We present, through figures 6–11, the DCS for the spin forbidden transitions from the metastable 2^3S state of helium to its singlet excited states, 2^1S, 2^1P, 3^1S, 3^1P, 4^1S, 4^1P. Since there are no theoretical or experimental cross sections comparable with the present calculation, we report our calculations in the three models (II, IF and FF) and the results of the first-Born type calculations (i.e. BOA and OA).

There is a qualitative similarity in the angular dependence of the DCS for the transitions 2^3S–3^1P and those for 2^3S–4^1P. The DCS for the transitions 2^3S–3^1S and 2^3S–4^1S differ somewhat from each other. The triplet–singlet (TS) transition in the present system (e + He) is caused by the electron exchange interaction. This gives rise to the following

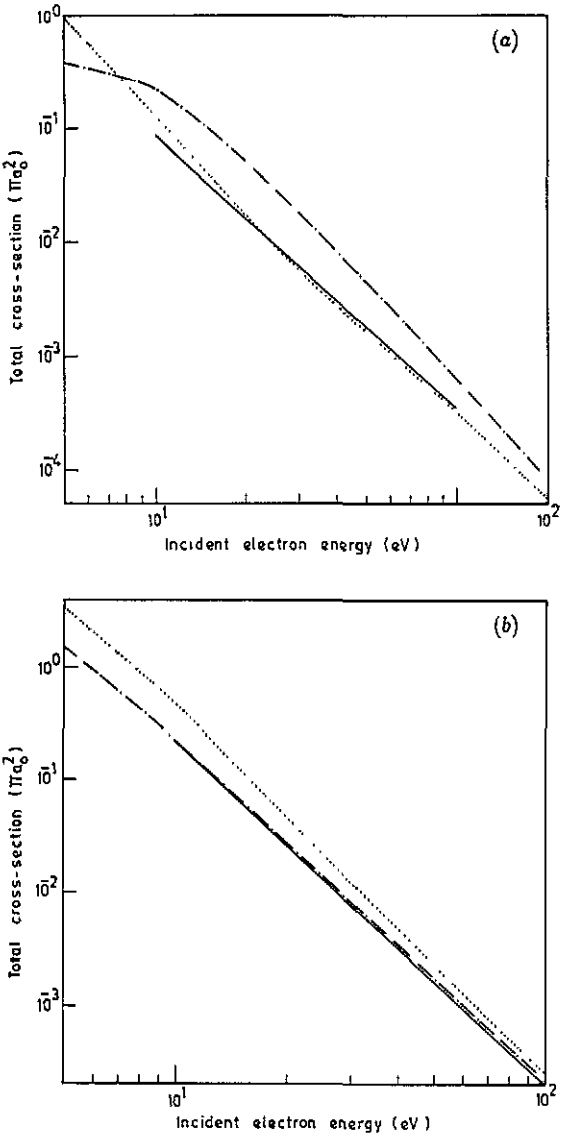

Figure 15. (*a*) TCS (πa_0^2) for 2^3S–3^1S excitation in helium. As in figure 14(*a*). (*b*) As in figure 15(*a*) but for 2^3S–3^1P excitation. (*c*) As in figure 15(*a*) but for 2^3S–4^1S excitation. (*d*) As in figure 15(*a*) but for 2^3S–4^1P excitation.

distinctive feature of the DCS *compared to those for the triplet–triplet* (TT) *transition.* First, the DCS for the TS process has a fairly large value in the region of large angles, while the TT cross section is very small there. Secondly, for the ^3S–^1P transitions, DCS has maximum at around 30° (not at 0° as in the case of ^3S–^3P transitions). In the TS case, the cross section in the IIP model is calculated with the parameter $\beta = 1$.

3.2. Total cross section

Figures 12 and 13 show the results of the TCS (in the FF model for the transitions 2^3S–n^3L ($n = 2, 3, 4$ and $L = 0, 1$). The results are obtained up to 100 eV the incident electron

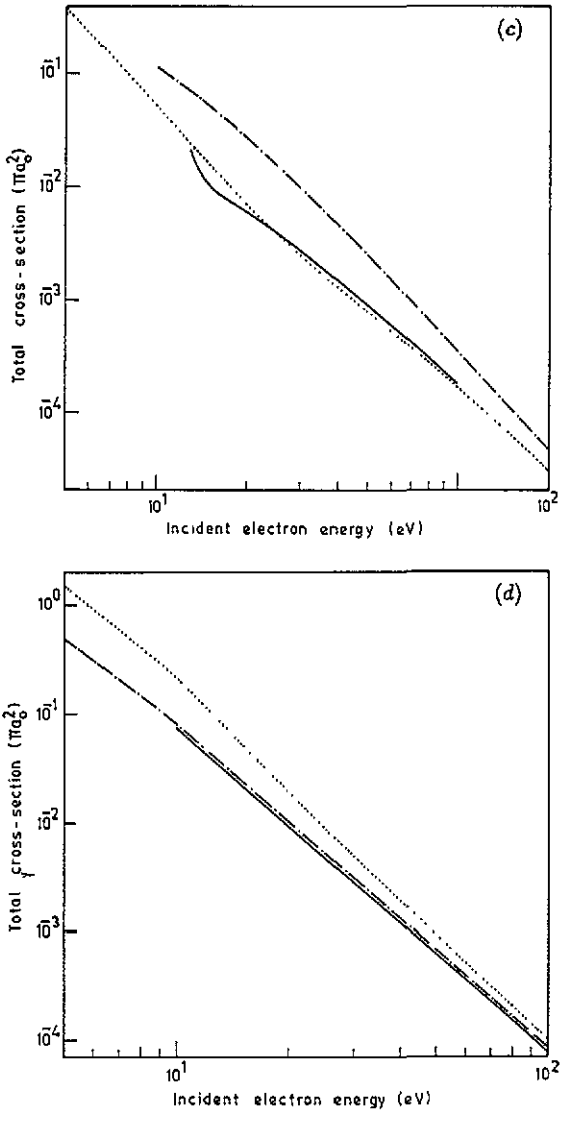

Figure 15. (continued)

energy and compared with other data as far as available. Also shown are the cross sections of our FBA calculation, which are slightly different from the previous FBA cross sections of Kim and Inokuti (1969) and Ton That *et al* (1977).

In figures 12(*a–c*), the TCS for the transitions 2^3S–2^3P, 2^3S–3^3S and 2^3S–3^3P are presented and compared with the theoretical cross sections of the FOMBT of Csanak *et al* (1994), the DWA of Mathur *et al* (1987), the DMET of Mansky and Flannery (1992) and the *R*-matrix method of Fon *et al* (1981) and Berrington *et al* (1985). For the excitations of 3^3S and 3^3P states, experimental data of Rall *et al* (1989) are also shown. It should be noted that the experimental data for 3^3S are apparent cross sections, which include cascade effects.

There are some discrepancies among different theoretical calculations, particularly for the excitation of the 3^3P state. The agreement between theory and experiment is

also poor. Figures 2 and 3 show that different theories give very different DCS in magnitude at the scattering angles larger than 30°. This makes the difference in TCS. There are no experimental data to determine which is the best calculation. The FBA calculation gives almost the same values of TCS as the present DWA calculation at energies above 10 eV. This seems peculiar if we consider the large difference shown in the figures of DCS.

In figures 13(*a*), (*b*), the TCS results of our FF model and the FBA calculation are presented for the 2^3S–4^3S and 2^3S–4^3P excitations. These results are compared with the only available result of Ochkur and Bratsev (1966). It is seen that our FBA and DWA results are lower than those of Ochkur and Bratsev even at 100 eV.

The TCS for the triplet–singlet excitations are given in figures 14 and 15. In figures 14(*a*), (*b*) the TCS for the transitions 2^3S–2^1S and 2^3S–2^1P are presented and compared with those of Badnell *et al* (1984) and Fon *et al* (1981). All the results obtained by our BOA, OA and DWA calculations tend to merge with the *R*-matrix result of Fon *et al* (1981) as the energy increases. In figure 15, we show our results for the 2^3S–3^1S, 2^3S–3^1P, 2^3S–4^1S, 2^3S–4^1P transitions. The present BOA cross sections are very close to our DWA ones even at lower energies.

Further, we compared our TCS results obtained using the three different DWA models among themselves (not shown here). We find that except for n^3P ($n=2$–4) excitations the results for each excitation show the behaviour that while they differ at low energies they tend to merge at high energies. However, for n^3P ($n=2$–4) excitations the merging seems to be at much higher energies. In the light of the non-availability of experimental data for most of the excitations considered here as well as in order to not discriminate among the three different DWA models we have given the TCS for all the $n^{3,1}L$ ($n=2$–4, $L=0$, 1) excitations using FF, IF and II models in tables 1–3.

4. Conclusion

We have carried out systematic calculations of the DCS and TCS for the electron impact excitation of helium from its metastable state 2^3S to higher excited states $n^{1,3}L$ ($n=2$–4, $L=0$, 1). This calculation has been performed in the three versions (II, IF, FF) of the distorted wave approximation proposed. The effect of polarization interaction is also studied in the II model resulting in the IIP cross section. We also carried out the first Born type calculation for comparison. The results of the DCS for the 2^3S–2^3P, 2^3S–3^3S, 2^3S–3^3P excitation are compared with the available experimental data. An overall agreement with those experimental data is generally good. Further our calculation suggests that the inclusion of the polarization potential may have a significant effect in some cases. To clarify this effect, we need more studies of the polarization interaction of excited atoms. We also compare our cross sections with other theoretical results available so far. Difference in the different calculations is found to be small.

The total cross section has been calculated up to 100 eV. For the excitations of 2^3P, 3^3S, 3^3P, 2^1S, 2^1P, the present cross sections are compared with the calculations of other authors. Except for a few special cases, the different calculations give almost the same values of the TCS. The theoretical cross sections, however, cannot reproduce the experimental TCS for the excitations of 3^3S and 3^3P states. It should be noted finally that the TCS obtained in the first Born type calculation is generally close to that obtained in the DWA calculation. This is very interesting, if we consider the large difference in

Table 1. Total cross section for transitions 2^3S-$n^{3,1}L$ ($n=2$-4, $L=0$, 1) in the FF version of DWA (in units of πa_0^2).

E_i (eV)	2^3S-2^3P	2^3S-3^3S	2^3S-3^3P	2^3S-4^3S	2^3S-4^3P	2^3S-2^1S	2^3S-2^1P	2^3S-3^1S	2^3S-3^1P	2^3S-4^1S	2^3S-4^1P
10	1.2 (+2)†	2.97 (00)	8.43 (−1)	4.17 (−1)	2.57 (−1)	2.18 (00)	1.92 (00)	7.79 (−2)	2.25 (−1)	1.49 (−2)	7.85 (−2)
15	8.72 (+1)	2.09 (00)	8.14 (−1)	2.96 (−1)	2.14 (−1)	1.06 (00)	6.25 (−1)	2.71 (−2)	6.12 (−2)	7.48 (−3)	2.23 (−2)
20	7.20 (+1)	1.61 (00)	7.69 (−1)	2.29 (−1)	2.09 (−1)	6.12 (−1)	1.84 (−1)	1.36 (−2)	2.55 (−2)	4.57 (−3)	9.33 (−3)
30	5.41 (+1)	1.10 (00)	6.91 (−1)	1.57 (−1)	1.88 (−1)	2.78 (−1)	5.16 (−2)	5.37 (−3)	7.49 (−3)	2.18 (−3)	2.78 (−3)
40	4.35 (+1)	8.31 (−1)	6.33 (−1)	1.20 (−1)	1.74 (−1)	1.47 (−1)	2.14 (−2)	2.80 (−3)	3.18 (−3)	1.22 (−3)	1.19 (−3)
50	3.57 (+1)	6.68 (−1)	5.45 (−1)	9.63 (−2)	1.58 (−1)	9.02 (−2)	1.08 (−2)	1.68 (−3)	1.64 (−3)	7.86 (−4)	6.14 (−4)
60	3.00 (+1)	5.59 (−1)	4.96 (−1)	8.06 (−2)	1.45 (−1)	5.80 (−2)	6.25 (−3)	1.11 (−3)	9.55 (−4)	5.33 (−4)	3.59 (−4)
70	2.57 (+1)	4.80 (−1)	4.57 (−1)	6.93 (−2)	1.32 (−1)	4.21 (−2)	3.92 (−3)	7.71 (−4)	5.89 (−4)	3.80 (−4)	2.28 (−4)
80	2.24 (+1)	4.21 (−1)	4.28 (−1)	6.08 (−2)	1.22 (−1)	3.08 (−2)	2.63 (−3)	5.62 (−4)	3.94 (−4)	2.81 (−4)	1.54 (−4)
90	1.98 (+1)	3.75 (−1)	4.15 (−1)	5.41 (−2)	1.14 (−1)	2.33 (−2)	1.84 (−3)	4.23 (−4)	2.78 (−4)	2.15 (−4)	1.09 (−4)
100	1.77 (+1)	3.37 (−1)	3.96 (−1)	4.88 (−2)	1.07 (−1)	1.79 (−2)	1.34 (−3)	3.28 (−4)	2.03 (−4)	1.68 (−4)	7.51 (−5)

† Entry in brackets shows the power of ten by which the value is to be multiplied.

Table 2. Total cross section for transitions 2^3S-$n^{3,1}L$ ($n=2$-4, $L=0$, 1) in the IP version of DWA (in units of πa_0^2).

E_i (eV)	2^3S-2^3P	2^3S-3^3S	2^3S-3^3P	2^3S-4^3S	2^3S-4^3P	2^3S-2^1S	2^3S-2^1P	2^3S-3^1S	2^3S-3^1P	2^3S-4^1S	2^3S-4^1P
10	1.18 (+2)	3.53 (00)	1.09 (00)	5.23 (−1)	4.26 (−1)	1.80 (00)	2.16 (00)	7.67 (−2)	3.90 (−1)	1.19 (−2)	1.57 (−1)
15	8.68 (+1)	2.32 (00)	8.75 (−1)	3.37 (−1)	2.77 (−1)	9.68 (−1)	4.87 (−1)	2.70 (−2)	8.00 (−2)	7.37 (−3)	3.16 (−2)
20	6.88 (+1)	1.73 (00)	7.94 (−1)	2.51 (−1)	2.47 (−1)	5.78 (−1)	1.87 (−1)	1.39 (−2)	2.97 (−2)	4.83 (−3)	1.15 (−2)
30	4.85 (+1)	1.15 (00)	6.90 (−1)	1.66 (−1)	2.05 (−1)	2.61 (−1)	5.20 (−2)	5.63 (−3)	8.12 (−3)	2.36 (−3)	3.11 (−3)
40	3.41 (+1)	8.59 (−1)	6.25 (−1)	1.24 (−1)	1.79 (−1)	1.43 (−1)	2.14 (−2)	2.93 (−3)	3.36 (−3)	1.34 (−3)	1.28 (−3)
50	2.66 (+1)	6.83 (−1)	1.15 (−1)	9.94 (−2)	1.65 (−1)	8.84 (−2)	1.09 (−2)	1.79 (−3)	1.71 (−3)	8.41 (−4)	5.09 (−4)
60	2.54 (+1)	5.71 (−1)	4.87 (−1)	8.27 (−2)	1.39 (−1)	5.89 (−2)	6.26 (−3)	1.15 (−3)	9.89 (−4)	5.66 (−4)	3.76 (−4)
70	2.13 (+1)	4.89 (−1)	4.48 (−1)	7.09 (−2)	1.27 (−1)	4.14 (−2)	3.93 (−3)	8.00 (−4)	6.06 (−4)	4.02 (−4)	2.46 (−4)
80	1.95 (+1)	4.28 (−1)	4.09 (−1)	6.20 (−2)	1.17 (−1)	3.03 (−2)	2.63 (−3)	5.82 (−4)	4.18 (−4)	2.96 (−4)	1.59 (−4)
90	1.70 (+1)	3.80 (−1)	3.77 (−1)	5.51 (−2)	1.07 (−1)	2.29 (−2)	1.85 (−3)	4.38 (−4)	2.94 (−4)	2.25 (−4)	1.12 (−4)
100	1.66 (+1)	3.42 (−1)	3.54 (−1)	4.96 (−2)	1.03 (−1)	1.78 (−2)	1.35 (−3)	3.38 (−4)	2.15 (−4)	1.75 (−4)	8.17 (−5)

Table 3. Total cross section for transitions 2^3S-$n^{3,1}L$ (n=2-4, L=0, 1) in the II version of DWA (in units of πa_0^2).

E_i (eV)	2^3S–2^3P	2^3S-3^3S	2^3S–3^3P	2^3S–4^3S	2^3S–4^3P	2^3S-2^1S	2^3S-2^1P	2^3S-3^1S	2^3S-3^1P	2^3S-4^1S	2^3S-4^1P
10	1.2 (+2)	2.67 (00)	7.10 (00)	3.99 (−1)	4.63 (−1)	1.60 (00)	2.51 (00)	1.44 (−1)	9.91 (−1)	2.39 (−2)	5.52 (−1)
15	8.72 (+1)	1.94 (00)	8.22 (−1)	2.70 (−1)	2.19 (−1)	9.30 (−1)	5.29 (−1)	3.66 (−2)	1.31 (−1)	8.60 (−3)	6.09 (−2)
20	7.20 (+1)	1.53 (00)	7.67 (−1)	2.14 (−1)	2.02 (−1)	5.67 (−1)	1.99 (−1)	1.74 (−2)	4.11 (−2)	5.64 (−3)	1.76 (−2)
30	5.41 (+1)	1.07 (00)	7.23 (−1)	1.51 (−1)	1.84 (−1)	2.58 (−1)	5.41 (−2)	6.49 (−3)	9.91 (−3)	2.69 (−3)	4.01 (−3)
40	3.41 (+1)	8.15 (−1)	6.32 (−1)	1.17 (−1)	1.65 (−1)	1.42 (−1)	2.21 (−2)	3.26 (−3)	3.88 (−3)	1.49 (−3)	1.46 (−3)
50	2.67 (+1)	6.59 (−1)	5.92 (−1)	9.45 (−2)	1.53 (−1)	8.75 (−2)	1.11 (−2)	1.91 (−3)	1.91 (−3)	9.18 (−4)	7.11 (−4)
60	2.55 (+1)	5.52 (−1)	4.95 (−1)	7.94 (−2)	1.41 (−1)	5.83 (−2)	6.38 (−3)	1.23 (−3)	1.09 (−3)	6.11 (−4)	4.25 (−4)
70	2.14 (+1)	4.75 (−1)	4.82 (−1)	6.85 (−2)	1.33 (−1)	4.10 (−2)	4.00 (−3)	8.51 (−4)	6.59 (−4)	4.29 (−4)	2.63 (−4)
80	1.95 (+1)	4.17 (−1)	4.17 (−1)	6.02 (−2)	1.23 (−1)	3.00 (−2)	2.67 (−3)	6.14 (−4)	4.48 (−4)	3.14 (−4)	1.74 (−4)
90	1.70 (+1)	3.71 (−1)	4.06 (−1)	5.36 (−2)	1.15 (−1)	2.27 (−3)	1.87 (−3)	4.59 (−4)	3.51 (−4)	2.37 (−4)	1.20 (−4)
100	1.62 (+1)	3.35 (−1)	3.61 (−1)	4.84 (−2)	1.08 (−1)	1.76 (−2)	1.59 (−3)	3.50 (−4)	2.23 (−4)	1.84 (−4)	8.79 (−5)

the corresponding DCS. We also hope that the tabulated form of the TCS data would be useful in various applications as well as for the purpose of future comparisons.

Acknowledgments

We are grateful to the Council of Scientific and Industrial Research (CSIR), New Delhi, India for financially supporting the present work. One of us (SV) is also grateful to CSIR, New Delhi, for the award of a Junior Research Fellowship.

References

Badnell N R 1984 *J. Phys. B: At. Mol. Phys.* **17** 4013–32
Berrington K A, Burke P G, Freitas L C G and Kingston A E 1985 *J. Phys. B: At. Mol. Phys.* **18** 4135–47
Burke P G 1993 *Proc. 18th Int. Conf. on Physics of Electronic and Atomic Collisions (Aarhus)* ed T Andersen, B Fastrup, F Folkman, H Knudsen and N Andersen (New York: American Institute of Physics) pp 26–47
Christophorou L G and Illenberger E 1993 *Phys. Lett.* **173A** 78
Csanak G, Cartwright D C and da Paixão F J 1994 private communication
Fon W C, Berrington K A, Burke P G and Kingston A E 1981 *J. Phys. B: At. Mol. Phys.* **14** 2921–34
Franca A and da Paixão F J 1994 *J. Phys. B: At. Mol. Opt. Phys.* **27** 1577–88
Furness J B and McCarthy I E 1973 *J. Phys. B: At. Mol. Phys.* **6** 2280–91
Itikawa Y 1986 *Phys. Rep.* **143** 69–108
Jhanwar B L and Khare S P 1976 *J. Phys. B: At. Mol. Phys.* **9** L527–9
Katiyar A K and Srivastava R 1989 *J. Phys. B: At. Mol. Opt. Phys.* **22** 1253–61
Kato T, Itikawa Y and Sakimoto K 1992 *Compilation of excitation cross sections for He atoms by electron impact* A research report from National Institute for Fusion Science, Nagoya, Japan (NIFS-DATA-15)
Khurana I, Srivastava R and Tripathi A N 1987 *J. Phys. B: At. Mol. Phys.* **20** 3515–30
Kim Y K and Inokuti M 1969 *Phys. Rev.* A **181** 205–14
Krishnan U and Stumpf B 1992 *At. Data. Nucl. Data Tables* **51** 151–69
Lin C C and Anderson L W 1992 *Adv. At. Mol. Opt. Phys.* **29** 1
Lockwood R B, Starpton F A, Andersen L W and Lin C C 1992 *Phys. Lett.* **166A** 357–60
Madison D H, Bartschat K and Srivastava R 1991 *J. Phys. B: At. Mol Opt. Phys.* **24** 1839–50
Mansky E J and Flannery M R 1992 *J. Phys. B: At. Mol. Opt. Phys.* **25** 1591–7
Mathur K C, McEachran R P, Parcell L A and Stauffer A D 1987 *J. Phys. B: At. Mol. Phys.* **20** 1599–608
Miller T M and Bederson B 1977 *Adv. At. Mol. Phys.* **13** 1–55
Mittleman M H and Watson K M 1960 *Ann. Phys., NY* **10** 268–79
Mott N F and Massey H S W 1965 *The Theory of Atomic Collisions* (Oxford: Oxford University Press)
Müller-Fiedler R, Schlemmer P, Jung K, Hotop H and Ehrhadt H 1984 *J. Phys. B: At. Mol. Phys.* **17** 259–68
Nakanishi H and Schrader D M 1986 *Phys. Rev.* A **34** 1810
Ochkur V I and Bratsev V F 1966 *Sov. Astron.* **9** 797–9
Rall D L A, Sharpton F A, Schulman M B, Anderson L W, Lawler J E and Lin C C1989 *Phys. Rev. Lett.* **62** 2253–6
Salvat F, Mayol R and Martinaz J D 1987 *J. Phys. B: At. Mol. Phys.* **20** 6597–612
Schiff L I 1968 *Quantum Mechanics* (New York: McGraw-Hill) p 377
Ton That D, Manson S T and Flannery M R 1977 *J. Phys. B: At. Mol. Phys.* **10** 621–35
Trajmar S and Nickel J C 1992 *Adv. At. Mol. Phys.* **30** 45–103
Verma S and Srivastava R 1994 *Hyperfine Int.* **89** 469–76
Vučić S, Potvliege R M and Joachain C J 1987 *J. Phys. B: At. Mol. Phys.* **20** 3157–69
Winter T G and Lin C C 1975 *Phys. Rev.* A **12** 434–43